

Discovery of a z=4.93, X-ray selected quasar by the Chandra Multiwavelength Project (ChamP)

John D. Silverman^{1,2,3}, Paul J. Green, Dong-Woo Kim, Belinda J. Wilkes, Robert A. Cameron, David Morris, Anil Dosaj²

Harvard-Smithsonian Center for Astrophysics, 60 Garden Street, Cambridge, MA 02138

Chris Smith

*Cerro Tololo Inter-American Observatory, National Optical Astronomy Observatory,
Casilla 603, La Serena, Chile*

Leopoldo Infante⁴

*Departamento de Astronomía y Astrofísica, P. Universidad Católica, Casilla 306, Santiago,
Chile*

Paul S. Smith

Steward Observatory, The University of Arizona, Tucson, AZ 85721

Buell T. Jannuzi

National Optical Astronomy Observatory, P.O. Box 26732, Tucson, AZ, 85726-6732

Smita Mathur

*Astronomy Department, Ohio State University, 140 West 18th Avenue, Columbus, OH
43210*

ABSTRACT

¹Astronomy Department, University of Virginia, P.O. Box 3818, Charlottesville, VA, 22903-0818

²Visiting Astronomer, Cerro Tololo Inter-American Observatory, National Optical Astronomy Observatory, which is operated by the Association of Universities for Research in Astronomy, Inc. (AURA) under cooperative agreement with the National Science Foundation.

³email: jds@head-cfa.harvard.edu

⁴Visiting astronomer, ESO New Technology Telescope

We present X-ray and optical observations of CXOMP J213945.0-234655, a high redshift ($z = 4.93$) quasar discovered through the Chandra Multiwavelength Project (ChaMP). This object is the most distant X-ray selected quasar published, with a rest-frame X-ray luminosity of $L_X = 5.9 \times 10^{44}$ erg s $^{-1}$ (measured in the 0.3–2.5 keV band and corrected for Galactic absorption). CXOMP J213945.0-234655 is a g' dropout object (> 26.2), with $r' = 22.87$ and $i' = 21.36$. The rest-frame X-ray to optical flux ratio is similar to quasars at lower redshifts and slightly X-ray bright relative to $z > 4$ optically-selected quasars observed with Chandra. The ChaMP is beginning to acquire significant numbers of high redshift quasars to investigate the X-ray luminosity function out to $z \sim 5$.

Subject headings: galaxies:active—galaxies:nuclei—quasars:general—quasars:individual (CXOMP J213945.0-234655)—X-rays:general

1. Introduction

The observed characteristics of known quasars are remarkably similar over a broad range of redshift. For example, X-ray studies utilizing the ROSAT database (Green et al. 1995; Kaspi et al. 2000), show little variation of the ratio of X-ray to optical flux for optically selected quasars. Also, the rest frame UV spectra of quasars, including the broad Ly α , NV and CIV emission lines, are nearly identical for a large range of redshift and present no evidence for subsolar metallicities even up to a $z \sim 6$ (Fan et al. 2001).

Even though the individual properties of quasars are similar, the co-moving space density of quasars changes drastically with redshift. At high redshift ($z > 4$), a significant dropoff in the co-moving space density of quasars seen in optical (e.g., Schmidt et al. 1995; Warren et al. 1994; Osmer 1982) and radio surveys (Shaver et al. 1996) hints at either the detection of the onset of accretion onto supermassive black holes or a missed high-redshift population, possibly due to obscuration. X-ray selected quasars from ROSAT have been used to support the latter interpretation based on evidence for constant space densities beyond a redshift of 2 (Miyaji et al. 2000). Unfortunately, the ROSAT sample size is small with only 8 quasars beyond a redshift of 3.

Significant numbers of quasars with $z > 4$ are being amassed to investigate both their intrinsic properties and the evolutionary behavior of the quasar population. The Sloan Digital Sky Survey (SDSS) reports 123 optically selected quasars with $z > 4$ (Schneider et al. 2001; Anderson et al. 2001). However, optical surveys suffer from selection effects due to intrinsic obscuration and the intervening Ly α forest. Current X-ray surveys with Chandra

and XMM do not have a strong selection effect based on redshift and can detect emission up to 10 keV (observed frame) to reveal hidden populations of active galactic nuclei (AGN) including heavily obscured quasars (Norman et al. 2001; Stern et al. 2001). High- z objects can be detected through a larger intrinsic absorbing column of gas and dust because the observed-frame X-ray bandpass corresponds to higher energy, more penetrating X-rays at the source.⁵ Therefore, optical and X-ray surveys will complement each other, providing a fair census of mass accretion onto black holes at high redshift.

Larger samples of X-ray observations of $z > 4$ quasars are needed since there are currently only 24 (Vignali et al. 2001), of which only 3 are X-ray selected quasars. Chandra and XMM-Newton are beginning to probe faint flux levels for the first time to detect the high- z quasar population. Initial Chandra and XMM-Newton observations of optically selected quasars have shown a systematically lower X-ray flux relative to the optical at high redshift (Vignali et al. 2001; Brandt et al. 2001a).

In this paper, we present the X-ray and optical properties of a newly discovered, X-ray selected $z = 4.93$ quasar with the Chandra Observatory. This quasar is the highest redshift object published⁶ from an X-ray survey.

These results are a component of the Chandra Multiwavelength Project (ChaMP; Wilkes et al. 2001). A primary aim of the ChaMP is to measure the intrinsic luminosity function of quasars and lower luminosity AGN out to $z \sim 5$. The survey will provide a medium-depth, wide-area sample of serendipitous X-ray sources from archival Chandra fields in Cycles 1 and 2 covering ~ 14 deg². The broadband sensitivity between 0.3–8.0 keV enables the selection to be far less affected by absorption than previous optical, UV, or soft X-ray surveys. Chandra’s small point spread function ($\sim 1''$ resolution on-axis) and low background allow sources to be detected to fainter flux levels, while the $\sim 1''$ X-ray astrometry greatly facilitates unambiguous optical identification of X-ray counterparts. The project will effectively bridge the gap between flux limits achieved with the Chandra deep field observations and those of past ROSAT surveys.

Throughout this paper, we assume $H_0 = 50$ km s⁻¹ Mpc⁻¹ and a flat cosmology with $q_0 = 0.5$.

⁵The observed-frame, effective absorbing column is $N_H^{\text{eff}} \sim N_H / (1 + z)^{2.6}$ (Wilman & Fabian 1999).

⁶A $z \sim 5.2$, X-ray selected quasar detected in the CDF-N was presented at the 199th AAS meeting (Brandt 2001b).

2. Observations and data analysis

2.1. X-ray

The X-ray source CXOMP J213945.0-234655 (Seq. 800104) was observed on November 18, 1999 by Chandra (Weisskopf et al. 2000) with the Advanced CCD Imaging Spectrometer (ACIS-I; Nousek et al. 1998) in the field of the X-ray cluster MS 2137.3-2353 (M. Wise, PI). We have used data reprocessed (in April 2001) at CXC⁷. We then ran a detection algorithm XPIPE (Kim et al. 2002) which was specifically designed for the ChaMP to produce a uniform and high quality source catalog.

CXOMP J213945.0-234655 is one of 72 sources detected using CIAO/wavdetect (Freeman et al. 2002) within the ACIS configuration (Figure 1). The 41 ksec observation yielded a net 16.7 ± 7.5 counts within the soft bandpass (0.3–2.5 keV) and no counts in the hard bandpass (2.5–8.0 keV). This corresponds to a Galactic absorption corrected, observed frame X-ray flux of $f(0.3 - 2.5 \text{ keV}) = 2.82 \pm 1.26 \times 10^{-15} \text{ erg cm}^{-2} \text{ s}^{-1}$ (Table 1).

The source naming convention of the ChaMP (CXOMP Jhhmmss.s±ddmmss) is given with a prefix CXOMP (Chandra X-ray Observatory Multiwavelength Project) and affixed with the truncated J2000 position of the X-ray source after a mean field offset correction is applied, derived from the cross-correlation of optical and X-ray sources in each field.

2.2. Optical Imaging and source matching

We obtained optical imaging of the field in three NOAO/CTIO SDSS filters (g', r' and i' ; Fukugita et al. 1996) with the CTIO 4m/MOSAIC on October 29, 2000 as part of the ChaMP optical identification program (Green et al. 2002). Integration time in each band ranged from 12–15 minutes during seeing of $1.3''$ – $1.8''$ FWHM. Image reduction was performed with the IRAF(v2.11)/MSCRED package. We used SExtractor (Bertin & Arnouts 1996) to detect sources, and measure (pixel) positions and magnitudes. Landolt standard stars were transformed to the SDSS photometric system (Fukugita et al. 1996) and used to calibrate the photometric solution. Following the convention of the early data release of the SDSS quasar catalog (Schneider et al. 2001), we present the optical photometry here as g^* , r^* and i^* since the SDSS photometry system is not yet finalized and the CTIO filters are not a perfect match to the SDSS filters. The limiting magnitudes for a point source are given as the mean of 3σ detections: $g^* = 26.18$, $r^* = 25.54$, $i^* = 25.11$.

⁷CXCDS versions R4CU5UPD14.1, along with ACIS calibration data from the Chandra CALDB 2.0b.

As evident from Figure 1, there are three optical sources detected down to a limiting i^* magnitude of 25.1 within the 50% encircled energy radius of the X-ray centroid. The two primary candidates, based on optical brightness, have offsets between the optical and X-ray positions of $1.87''$ and $4.94''$. To determine whether either of these sources are the likely counterpart to the X-ray detection, we have determined errors associated with the X-ray astrometric solution.

Kim et al. (2002) have carried out extensive simulations of point sources generated using the SAOSAC raytrace program (<http://hea-www.harvard.edu/MST/>) and detected using CIAO/`wavdetect`. For weak sources of ~ 20 counts between $8'-10'$, off-axis from the aim point, the reported X-ray centroid position is correct within $1.8''$, corresponding to a 1σ confidence contour. Therefore, the nearby optical source ($\Delta r=1.9''$) is the likely counterpart to the X-ray detection. The (J2000) position of the optical counterpart as measured from the r' image referenced to the Guide Star Catalog II⁸ is $\alpha = 21^h 39^m 44.99^s \delta = -23^\circ 46' 56.6''$.

2.3. Optical spectroscopy

We obtained a low resolution optical spectrum of CXOMP J213945.0-234655 (Figure 2) with the CTIO 4m/HYDRA multi-fiber spectrograph on October 15, 2001. Spectra of 17 of 22 optical counterparts to X-ray sources with a magnitude $r^* < 21$ were acquired in a three hour integration within the Chandra field. The spectrograph has $2''$ diameter fibers and was configured with a 527 l/mm grating that provided $\sim 2800 \text{ \AA}$ of spectral coverage with a resolution of $\sim 4 \text{ \AA}$. The sky background was measured using 81 fibers not assigned to the Chandra X-ray detections within the 1° field spectrograph. We processed the data using the IRAF(v2.11)/HYDRA reduction package.

An additional spectrum of the high redshift quasar (Figure 2) and the optically brighter source $4.9''$ west of the Chandra X-ray position were obtained on the following evening with the ESO/NTT 3.5m to verify the intriguing Hydra spectrum and obtain greater wavelength coverage. A 300 l/mm grating was implemented with a wavelength coverage of 4000 \AA and a resolution of $\sim 11 \text{ \AA}$. Due to poor weather conditions at the end of the evening, flux calibration was done using the standard star LTT 2415 observed the following night. From the NTT spectrum, we classify the brighter object as an M3 dwarf with no sign of emission lines, confirming the quasar as the optical counterpart of the X-ray source.

⁸The Guide Star Catalogue-II is a joint project of the Space Telescope Science Institute and the Osservatorio Astronomico di Torino.

We measured a mean redshift $z=4.930 \pm 0.004$ from the Ly β +OVI, CII, SiIV+OIV] and CIV emission lines in the NTT spectrum. Using this redshift, the Ly α line centroid is shifted by ≈ 4 Å redward from the expected rest wavelength, probably due to significant HI absorption. This is similar to the mean shift of Ly α observed in a sample of 33 high redshift quasars by Schneider et al. (1991).

The spectrum obtained at the NTT was used to measure the rest-frame equivalent widths of Ly β /OVI (30 ± 7 Å), Ly α +NV (73 ± 5 Å), and CIV (40 ± 8 Å). For comparison, we also measured Ly α +NV for 10 high redshift quasars in the range $4.8 < z < 5.1$ from the SDSS spectra of Anderson et al. (2001). This subsample has a similar mean redshift (4.91), but with an average $i^* = 19.7$ is 4.5x more optically luminous than CXOMP J213945.0-234655. Nevertheless, the mean rest-frame equivalent width of Ly α +NV in the SDSS subsample is consistent at 79 Å, with an RMS dispersion of 27 Å. The poor S/N of the SDSS spectra and the strong Ly α forest, prevent meaningful comparison of other line strengths.

3. Results

To compare the broad band spectral energy distribution of CXOMP J213945.0-234655 to other X-ray detected quasars, we have calculated α_{ox} (Tananbaum et al. 1979), the slope of a hypothetical powerlaw between the X-ray and optical flux. The rest-frame, monochromatic luminosity at 2 keV corresponding to the derived X-ray flux is $\log l_{2 \text{ keV}} = 26.76$ erg s $^{-1}$ Hz $^{-1}$. Assuming $\alpha=0.5$ for the optical continuum powerlaw slope, we derive the rest-frame, monochromatic optical luminosity at 2500 Å from the i^* magnitude to be $\log l_{2500\text{\AA}} = 30.73$ erg s $^{-1}$ Hz $^{-1}$. We thus find $\alpha_{ox} = 1.52^{+0.08}_{-0.05}$. Table 1 lists the measured X-ray and optical properties of CXOMP J213945.0-234655.

We compare the X-ray to optical flux ratio of CXOMP J213945.0-234655 to other $z > 4$ quasars by plotting the observed-frame, Galactic absorption corrected 0.5–2.0 keV X-ray flux versus the AB $_{1450(1+z)}$ magnitude (Figure 3). The plotted lines represent the locus of points for a hypothetical quasar with a wide range of luminosities and an $\alpha_{ox}=1.6 \pm 0.15$ (Green et al. 1995), representative of the mean for quasars selected from the Large Bright Quasar Survey and detected in the ROSAT All-Sky Survey. The α_{ox} of CXOMP J213945.0-234655 is comparable with low redshift quasars in contrast to the X-ray faint Chandra detections of optically selected quasars at $z > 4$ (Vignali et al. 2001). The X-ray weakness of the latter may be due to intrinsic absorption by large amounts of gas in the quasars’ host galaxies.

X-ray and optical observations of CXOMP J213945.0-234655 show no direct evidence of significant obscuration. The optical color ($r^* - i^* = 1.51 \pm 0.12$) is consistent with optically

selected quasars. We measured the mean color $r^* - i^*$ from 15 SDSS quasars (Anderson et al. 2001) with $4.7 < z < 5.2$ to be 1.69 with RMS dispersion of 0.30. The upper limit to the X-ray hardness ratio (< -0.54) hints at an unobscured X-ray spectrum, although a moderately absorbed component, if present, would be redshifted out of the Chandra bandpass.

X-ray selected samples may be less biased against absorbers (both intrinsic and line-of-sight) than are optically-selected samples, an advantage expected to be especially important at high redshifts. From our flux-calibrated NTT spectrum, we measure $D_A = (f_{cont} - f_{obs})/f_{cont}$, the flux decrement caused by the Ly α forest (Oke & Korycansky 1982) relative to an extrapolated power-law continuum⁹ in the region between rest-frame limits 1050–1170 Å. The value we measure of $D_A = 0.79 \pm 0.02$ is between the $\bar{z} \sim 4$ measurement of 0.54 from Rauch et al. (1997) and the $z \sim 6$ measurements of $D_A \sim 0.9$ from 4 SDSS quasars in Becker et al. (2001). While CXOMP J213945.0-234655 thus appears consistent with the handful of bracketing measurements of optically-selected quasars (see also Riediger et al. 1998), more high redshift X-ray selected quasars are needed to test possible biases caused by absorption.

CXOMP J213945.0-234655 exemplifies the potential for the ChaMP project to detect quasars with fluxes at the faint end of the $f_x - f_{opt}$ parameter space (Figure 3). This will allow the ChaMP to acquire significant numbers of high redshift quasars. From the first year of spectroscopic followup of Chandra X-ray sources to $i' \lesssim 21$, we currently have 22 newly identified quasars with $z > 2$ and eight with $z > 3$, approximately 2–3 such objects per field. Nearly 5% of ChaMP sources identified to date are $z > 3$ quasars.

4. Conclusion

We present the discovery of CXOMP J213945.0-234655, at $z = 4.93$ the most distant X-ray selected object published to date. With a measured optical to X-ray flux ratio $\alpha_{ox} = 1.52$, CXOMP J213945.0-234655 is similar to low redshift quasars, in contrast to several optically-selected $z > 4$ quasars previously detected by Chandra.

This detection highlights the importance of wide area, intermediate depth surveys like the ChaMP for studies of the high redshift quasar population ($z \sim 3$ to 5). The ChaMP¹⁰ has begun to amass a sample of high redshift, X-ray selected quasars with the goal of measuring

⁹As in Fan et al. (2001), we measure the observed flux f_{obs} relative to a $f_\lambda \propto \lambda^{-1.5}$ power-law continuum normalized to the observed flux in the region 1270 ± 10 Å in the rest-frame. We derive uncertainties by measuring against continua with slopes in the range $-0.5 < \alpha \leq 1.5$.

¹⁰<http://hea-www.harvard.edu/CHAMP/>

the cosmic evolution of accretion-powered sources relatively unhampered by the absorption and reddening that affects optical surveys.

We gratefully acknowledge support for this Chandra archival research from NASA grant AR1-2003X. RAC, AD, PJG, DK, DM, and BW also acknowledge support through NASA Contract NASA contract NAS8-39073 (CXC). LI is grateful to “Proyecto Puente PUC” and Center for Astrophysics FONDAP for partial financial support. BTJ acknowledges research support from the National Science Foundation, through their cooperative agreement with AURA, Inc., for the operation of the NOAO. We are thankful to Sam Barden and Tom Ingerson (NOAO) for building and commissioning Hydra/CTIO. We greatly appreciate the observing support from Knut Olsen (NOAO), and constructive comments by Harvey Tananbaum and Dan Harris.

REFERENCES

Anderson, S.F. et al. 2001, AJ, 122, 503
Becker et al. 2001, AJ, 122, 2850
Bertin, E. & Arnouts, S. 1996, A&AS, 117, 393
Brandt, W. N., Guainazzi, M., Kaspi, S., Fan, X., Schneider, D. P., Strauss, M. A., Clavel, J., Gunn, J. E. 2001a AJ, 121, 591
Brandt, W. N. 2001b, BAAS, 199, 148.03
Brandt, W.N. et al. 2001c, AJ, 122, 2810
Dickey & Lockman 1990, ARAA, 28, 215
Fan, X. et al. 2001, AJ, 122, 2833
Freeman, P. E., Kashyap, V., Rosner, R., Lamb, D. Q. 2002 ApJS, 138, in press (astro-ph/0108429)
Fukugita, M., Ichikawa, T., Gunn, J.E., Doi, M., Shimasaku, K., Schneider, D.P. 1996, AJ, 111, 1748
Green, P.J., Schartel, N., Anderson, S.F., Hewett, P.C., Foltz, C.B., Brinkmann, W., Fink, H., Trümper, J., Margon, B. 1995, ApJ, 450, 51

Green, P.J. et al. 2002, in preparation

Kaspi, S., Brandt, W.N., Schneider, D.P. 2000, AJ, 119, 2031

Kim, D.-W., et al. 2002, in preparation

Miyaji, T., Hasinger, G., Schmidt, M. 2000, A&A, 353, 25

Norman, C., et al. 2001, in press (astro-ph/0103198)

Nousek, J.A., et al. 1998, SPIE, 3444, 225

Oke, J. B., Korycansky, D.G 1982, ApJ, 255, 11

Osmer, P.S. 1982, ApJ, 253, 28

Schneider, D.P., Schmidt, M., Hasinger, G., Lehmann, I., Gunn, J.E., Giacconi, R., Trümper, J., Zamorani, G. 1998, AJ, 115, 1230

Rauch, M., Miralda-Escude, J., Sargent, W. L. W., Barlow, T. A., Weinberg, D. H., Hernquist, L., Katz, N., Cen, R., Ostriker, J. P. 1997, ApJ, 489, 7

Riediger, R. Petitjean, P., & Mücket, J. P. 1998, A&A, 329, 30

Schmidt, M., Schneider, D.P., Gunn, J.E. 1995, AJ, 110, 68

Schneider, D.P., Schmidt, M., Gunn, J.E. 1991, AJ, 101, 2004

Schneider et al., 2001, in pressss (astro-ph/0110629)

Shaver, P.A., Wall, J.V., Kellermann, K.I., Jackson, C.A., Hawkins, M.R.S. 1996, Nature, 384, 439

Stern, D., et al. 2001, in press (astro-ph/0111513)

Tananbaum, H., Avni, Y., Branduardi, G., Elvis, M., Fabbiano, G., Feigelson, E., Giacconi, R., Henry, J. P., Pye, J. P., Soltan, A., Zamorani, G 1979, ApJ, 234L, 9

Warren, S.J., Hewett, P.C., Osmer, P.S. 1994, ApJ, 421, 412

Weisskopf, M.C., Tananbaum, H.D., Van Speybroeck, L., P., O'Dell, S.L., 2000, SPIE, 4012, 2

Wilkes, B. J., et al. 2001, in ASP Conf. Ser. 232, New Era of Wide Field Astronomy, ed. R. G. Clowes, A. J. Adamson, & G. E. Bromage (San Francisco: ASP), 47

Wilman, R. J. & Fabian, A. C. 1999, ApJ, 522, 157

Vignali, C., Brandt, W.N., Fan, X., Gunn, J.E., Kaspi, S., Schneider, D.P., Strauss, M.A
2001, AJ, 122, 2143

Table 1. Properties of CXOMP J213945.0-234655

Parameter	Value	Parameter	Value
$\alpha_{\text{J}2000}$ ¹	21 39 44.99	X-ray counts ⁴	16.7 ± 7.5
$\delta_{\text{J}2000}$ ¹	-23 46 56.6	$f_X(\text{erg s}^{-1} \text{cm}^{-2})$ ^{3,4}	$(2.82 \pm 1.26) \times 10^{-15}$
z	4.930 ± 0.004	$L_X(\text{erg s}^{-1})$ ^{3,5}	$(5.89 \pm 2.63) \times 10^{44}$
g^*	>26.2	Hardness Ratio ⁶	< -0.54
r^*	22.87 ± 0.07	α_{ox}	$1.52^{+0.08}_{-0.05}$
i^*	21.36 ± 0.10	$AB_{1450(1+z)}$ ²	21.62

¹units RA (hms), DEC ($\circ / ''$); error <0.5''

²observed monochromatic, Galactic absorption corrected, $AB_{1450(1+z)}$ magnitude (Fukugita et al. 1996) emitted at 1450 Å in the quasar's rest-frame; based on an assumed optical powerlaw spectrum ($S_\nu \propto \nu^{-\alpha}$; $\alpha=0.5$)

³based on an assumed X-ray powerlaw spectrum ($S_E \propto E^{-\alpha}$; $\alpha=1.0$); Galactic absorption corrected ($N_H = 3.55 \times 10^{20} \text{ cm}^{-2}$; Dickey & Lockman 1990)

⁴observed-frame; 0.3–2.5 keV

⁵rest-frame; 0.3–2.5 keV

⁶(H-S)/(H+S); soft band(S): 0.3-2.5 keV, hard band(H): 2.5-8.0 keV

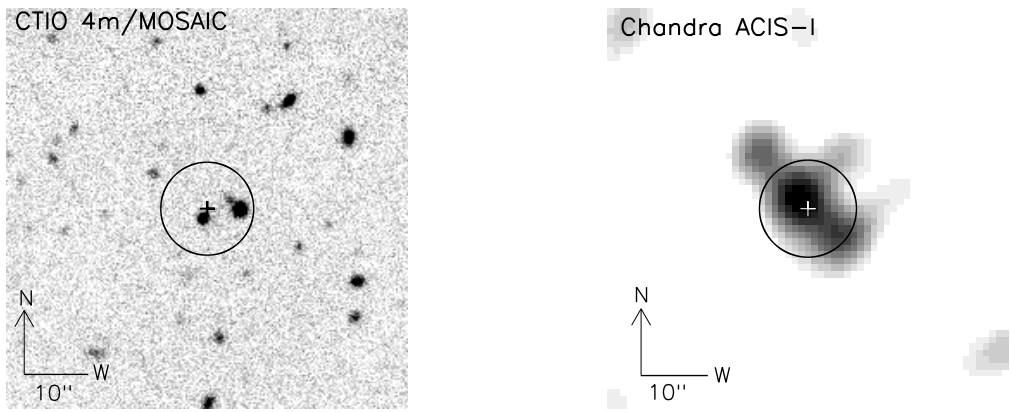


Fig. 1.— Optical (i') and X-ray (0.3–2.5 keV) imaging. To improve the visual clarity, in this figure we have smoothed the Chandra image with a gaussian function ($\sigma=1.5''$). The spatial distribution of the 17 X-ray counts at $9.1'$ off-axis is as expected from a point source. The black circle shows the region containing 50% of the encircled energy (radius= $7.3''$) of the Chandra counts. The cross marks the centroid of the X-ray emission in both images.

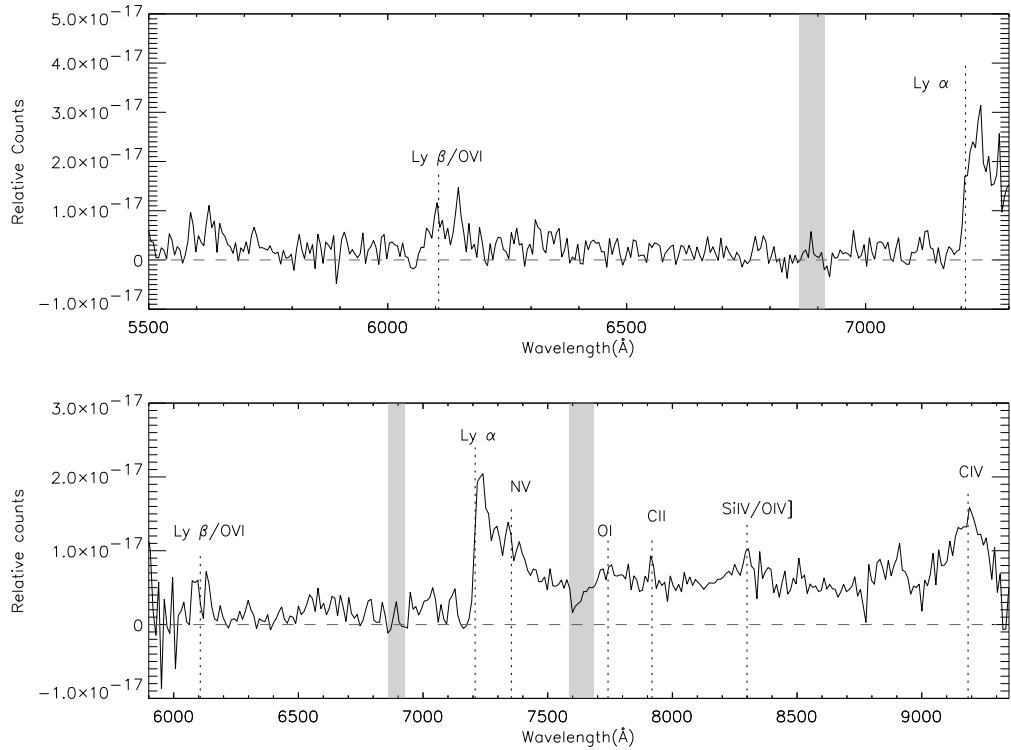


Fig. 2.— Optical Spectroscopy of CXOMP J213945.0-234655. The top spectrum is the discovery observation taken with the CTIO 4m/HYDRA on October 15, 2001. The spectrum has been binned to produce a resolution of 16.4 Å. The bottom figure is a followup observation with the NTT on the next evening to detect spectral features redward of Ly α (11 Å resolution). Dashed lines indicate the expected positions of emission lines at a redshift of 4.93. Shaded regions mark the uncorrected telluric O₂ absorption band regions.

